J Mol Model (2013) 19:4419–4432
DOI 10.1007/s00894-013-1956-z

ORIGINAL PAPER

Effects of trimethylaluminium and tetrakis(ethylmethylamino) hafnium in the early stages of the atomic-layer-deposition of aluminum oxide and hafnium oxide on hydroxylated GaN nanoclusters

Paola A. León-Plata · Mary R. Coan · Jorge M. Seminario

Received: 20 June 2013 / Accepted: 22 July 2013 / Published online: 7 August 2013
© Springer-Verlag Berlin Heidelberg 2013

Abstract We calculate the interactions of two atomic layer deposition (ALD) reactants, trimethylaluminium (TMA) and tetrakis(ethylmethylamino) hafnium (TEMAH) with the hydroxylated Ga-face of GaN clusters when aluminum oxide and hafnium oxide, respectively, are being deposited. The GaN clusters are suitable as testbeds for the actual Ga-face on practical GaN nanocrystals of importance not only in electronics but for several other applications in nanotechnology. We find that TMA spontaneously interacts with hydroxylated GaN; however it does not follow the atomic layer deposition reaction path unless there is an excess in potential energy introduced in the clusters at the beginning of the optimization, for instance, using larger bond lengths of various bonds in the initial structures. TEMAH also does not interact with hydroxylated GaN, unless there is an excess in potential energy. The formation of a Ga—N(CH_3)(CH_2CH_3) bond during the ALD of HfO_2 using TEMAH as the reactant without breaking the Hf—N bond could be the key part of the mechanism behind the formation of an interface layer at the HfO_2/GaN interface.

Keywords DFT · Dissociation · Interface layer · Nanoclusters · Wide bandgap semiconductor

P. A. León-Plata · M. R. Coan · J. M. Seminario
Department of Chemical Engineering, Texas A&M University, College Station, TX, USA

J. M. Seminario
Materials Science and Engineering Graduate Program, Texas A&M University, College Station, TX, USA

J. M. Seminario (✉)
Department of Electrical and Computer Engineering, Texas A&M University, College Station, TX, USA
e-mail: seminario@tamu.edu

Introduction

Nanotechnology provides excellent opportunities to develop all sorts of devices with tuned properties not only for electronics but practically for all areas of science and engineering. A straightforward way to reach these goals is to prepare nanoclusters whose properties depend strongly on their size and shape, in addition to their intrinsic characteristics of their component atoms and interactions. Currently, enhancement-mode (E-mode) III-V based devices are needed for low-loss high-power RF switching along with transmitter/receiver switches for global positioning system (GPS) receivers in mobile phones [1]. The achievement of E-mode III-V based devices, as high electron mobility transistors (HEMTs), is dependent on the ability to control the threshold voltage (V_{th}); one current method for this is using high-k metal gate stacks (that include high-k dielectrics such as AlO_2 and/or HfO_2), which can vary the work function of the gate metal and therefore the threshold voltage [2–4]. Previous work reported the formation of an interfacial layer at the atomic-layer-deposited (ALD) HfO_2–GaN interface [5, 6], while no interfacial layer has been found for ALD of Al_2O_3 on GaN [7, 8]. The formation of an interfacial layer at the semiconductor/dielectric interface can cause detrimental effects on the performance and the reproducibility of the device along with changes in the threshold voltage of the device. A better understanding of the mechanism responsible for the formation of an interfacial layer during the atomic layer deposition of HfO_2 on GaN would give us insights into determining the removal or the non-formation of the interfacial layer.

In this paper, the interactions of trimethylaluminium (TMA) and tetrakis(ethylmethylamino) hafnium (TEMAH) with the hydroxylated Ga-face of GaN clusters are studied using density functional theory (DFT) with the intent to improve the development of E-mode III-V based devices and to investigate the features of these devices as they are scaled down to nanosizes.

The first step in many atomic layer deposition processes is to introduce H_2O or another oxygen source to oxidize the surface of the sample; an example of this is the use of deionized water as a source of oxidizing agent [9, 10]. In order to fully understand the mechanisms of the atomic layer deposition process of HfO_2 and Al_2O_3, the oxidation of GaN surface must first be understood. Theoretical calculations of the interactions of O_2 and/or H_2O with GaN (0001) have previously been reported using density functional theory (DFT) within the generalized gradient approximation (GGA) [11, 12], and using hybrid functionals [13–15]. TMA and TEMAH are commonly used as precursors during the atomic layer deposition process of Al_2O_3 and HfO_2, respectively. The authors believe, forming individual devices with small nano-clusters could expand their applications beyond photonics and electronics areas such as catalysis, sensing [16], and biomedical applications. Recently, GaN nanoclusters have been made by using the sequential ion implantation on a dielectric matrix [17]. Another method to form GaN nanoclusters is to rinse the sample in a solution of a donor stabilized gallium-triazid [18]. These may be considered nanoclusters of GaN adsorbed over the surface of a thin film. Materials made from or containing GaN have been extensively studied since the early 1990s theoretically using ab initio electronic structure methods for GaN clusters [19–28]. The theoretical studies of structural, dielectric, phonon dispersions and density of states for wurzite and/or zinc-blende GaN along with the stoichiometry and structure of the (0001) surface of GaN have been reported [19, 21, 22]. The structural and electronic properties of GaN clusters have been previously modeled [23–25, 28].

Methodology

We use density functional theory [29, 30] with the B3PW91, which is a hybrid functional that uses the Becke exchange [31] combined with a Hartree-Fock [32–34] component and the correlation functional of Perdew-Wang [35–39]. This functional has been used successfully in a variety of applications involving related clusters of atoms [26, 40–42] and other applications involving molecular electronics devices [16, 43]. It has also been used in applications involving metallic clusters [44–50]. The basis set and effective core potential used together with the hybrid functional is the LANL2DZ [51–53], which has also been proved to yield acceptable theoretical predictions [16, 43, 54–57]. Optimizations are carried out with the Berny method [58, 59]. All of the optimized stable structures are checked to be local minima by calculating the Hessian matrix, i.e., the second derivative of the energy with respect to all coordinates. When we find that a structure yields negative Hessian eigenvalues, the geometry is modified accordingly in order to reach a stable structure. All of the DFT calculations are performed with the program GAUSSIAN-09 [60].

The reaction mechanisms of two atomic layer deposition reactants with hydroxylated GaN(0001) surface are studied using hexagonal wurzite crystal geometries that resemble bulk GaN with a=3.189 Å and c=5.186 Å [61]. Hexagonal wurzite crystal geometries are considered the most thermodynamically stable structures for GaN. The Ga surface of GaN has each Ga bonded to three N's and maintains one dangling bond perpendicular to the surface. The GaN clusters are hydroxylated using 1, 2 or 3 –OH groups bonded to the Ga of the surface. Three main surface structures are used to model hydroxylated bulk Ga-face GaN, Ga-centered, N-centered, and hollow-centered surface structures. Two different atomic layer deposition (ALD) reactants are used: trimethylaluminium (TMA) and tetrakis(ethylmethylamino)hafnium (TEMAH) (Fig. 1). TMA is used as the reactant in ALD when Al_2O_3 is being deposited, while TEMAH is used when HfO_2 is being deposited.

Calculations for the hydroxylated Ga-centered, N-centered, and hollow-centered surface clusters (Fig. 2) under the presence of an ALD reactants are calculated with varying multiplicities. In some cases atoms of the reactants and of the –OH group are shifted to induce interactions. Once a stable interaction between the ALD reactant and the hydroxylated GaN cluster occurs, further geometry optimizations are completed to investigate the formation of the Ga-O—Hf and Ga-O—Al bonds.

In the following two sections we discuss the cases when trimethylaluminium (TMA) is used as reactant when Al_2O_3 is deposited (ALD) on GaN and when tetrakis(ethylmethylamino)hafnium (TEMAH) is used as reactant when HfO_2 is deposited on GaN; therefore, we will focus on the interaction of reactants with the surface whereby a layer is formed in between the HfO_2 and the surface.

Trimethylaluminum reactant for aluminum oxide deposition on gallium nitride

The early steps of the deposition of Al_2O_3 on GaN using TMA is studied by finding stable structures of the complexes obtained by placing the TMA near the hydroxylated variants

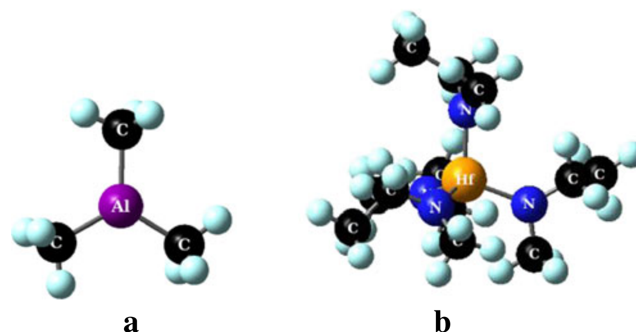

Fig. 1 **a** Trimethylaluminium (TMA) and **b** tetrakis(ethylmethylamino)hafnium (TEMAH). H: white, C: black, Al: purple, Hf: yellow

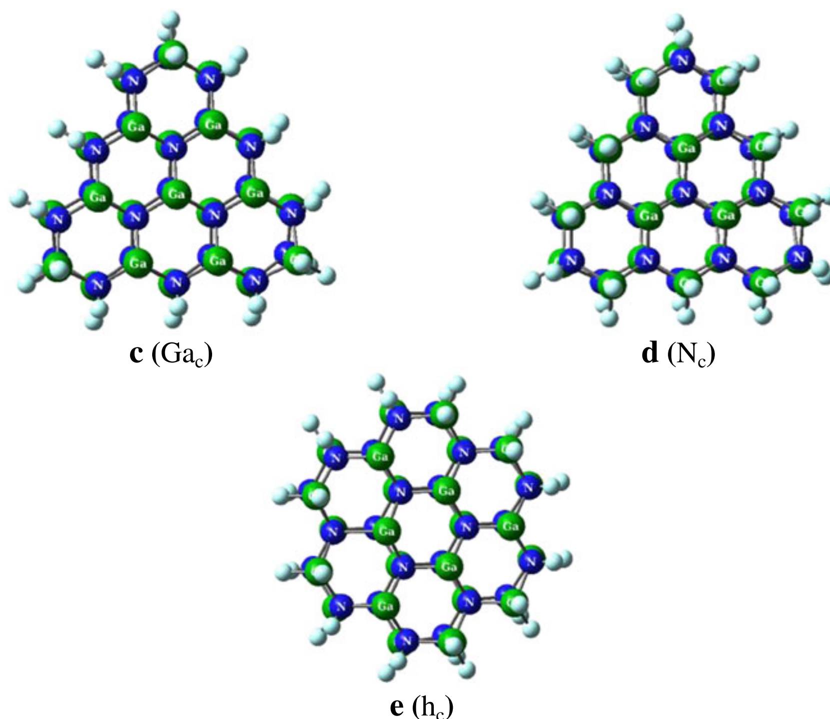

Fig. 2 Top views of optimized GaN clusters used as surface reactive centers of a GaN surface **c**: Ga-centered, **d:** N-centered and **e**: hollow centered. Ga: green, N: blue

of GaN. Three GaN models are used: the Ga-centered (Ga_c), N-centered (N_c) and hollow-centered (h_c). The ALD of Al_2O_3 on GaN is then represented in these optimized complexes (Fig. 3). The total energies are shown in Table 1 for all these complexes; only geometries tested that yield stable complexes are reported.

For the Ga_c cluster, the most common stable interaction between the TMA and $Ga_c(OH)$ leads to the bonding of the TMA to the OH group without breaking any bonds in the complex, $Ga_c(OH)$+TMA (**f**, **g**, **j**, **k**). However, the most stable interaction yields the formation of a CH_4 and an O—Al bond (**h**) starting from a TMA with a stressed Al—CH_3 bond of 2.63 Å rather than typical Al—C bond length in TMA of 1.99 Å [62], while the group OH length is 1.16 Å rather than the typical length of 0.98 Å.

These shifts in bond lengths are necessary to form a GaO—Al bond and a CH_4, which are believed to be the result of TMA reacting with an –OH group [63, 64]. Without shifting any atoms in the complex, the most stable interaction between TMA and $Ga_c(OH)$ has a final relative energy (E_R) of 0.78 eV (**f**).

The above procedure is repeated for the single TMA molecule placed now over the double and triple hydroxylated Ga_c cluster, $Ga_c(OH)_2$ and $Ga_c(OH)_3$, respectively, in several orientations and distances from the surface and optimized (**l-s**). The most stable interaction of TMA with either $Ga_c(OH)_2$ (**l**) or $Ga_c(OH)_3$ (**r**) leads to a bonding of the TMA to one of the –OH groups without breaking any bonds in the structure. However, other optimized geometries also reached similar structures with slightly higher energies (Table 1). The formation of CH_4 does not occur for any geometry tested, including non-stable geometries. None of the atoms are shifted to induce a reaction in the $Ga_c(OH)_2$ (**l-o**) or $Ga_c(OH)_3$ (**p-s**) geometries.

Then, Two TMA molecules are placed over the double and triple hydroxylated clusters, in several orientations and distances from the surface and then optimized (**t-y**). The most stable interaction of TMA with either $Ga_c(OH)_2$ (**t**) or $Ga_c(OH)_3$ (**x**) yields a bonding of each of the TMA molecules to one of the –OH groups without breaking any bonds in the complex. Likewise other optimized geometries also have similar structures with slightly higher energies (Table 1), and the formation of CH_4 does not occur for any geometry tested, including non-stable geometries. Atoms are shifted to induce a reaction in the $Ga_c(OH)_2$+2TMA (**u**) complex; however, shifting does not yield the formation of a CH_4, in fact, the geometry failed to converge.

For the N-centered GaN cluster, N_c, a single TMA is placed on a single and a triple hydroxylated $N_c(OH)$ and $N_c(OH)_3$, respectively, in several orientations and distances from the surface. These complexes are then optimized (**z** and **aa**) and only the stable structures are shown. The only geometry that yields a stable bonded structure is $N_c(OH)_3$ (**aa**); this interaction leads to the bonding of TMA to one of the –OH groups without breaking any bonds in the TMA or the GaN cluster. The formation of CH_4 does not occur for any geometry tested, including non-stable geometries, which are not shown.

Similarly, for the hollow-centered GaN, h_c, a single TMA molecule is placed over the singly hydroxylated h_c cluster, $h_c(OH)$, in several orientations and distances from the surface and optimized(**ab-ad**). The most stable interaction yields the formation of an O—Al bond and a CH_4 (**ad**) from a TMA

(1, 0.78) **f**

(3, 1.08) **g**

(1, 0.00) **h** [—CH_3 shifted]

(1, 1.75) **i**

(1, 0.79) **j**

(3, 1.08) **k**

(2, 0.00) **l**

(4, 0.31) **m**

(2, 0.72) **n**

(4, 1.02) **o**

(1, 0.60) **p**

(3, 1.19) **q**

(1, 0.00) **r**

(3, 0.24) **s**

(2, 0.00) **t**

(2, 0.32) (osc) **u** [—CH_3 shifted]

Fig. 3 GaN-clusters (partially H-passivated) hydroxylated (with 1, 2 or 3–OH groups) final structures when optimized under the presence of one or two TMA molecules. The complexes are labeled with (m, E_R), indicating their spin multiplicity (m), and relative energy in eV (E_R) with respect to the most stable conformation, and bold letters; chemical changes with respect to their initial geometries are indicated inside square brackets. For Ga_c GaN clusters, **f**–**k** (started from Ga_c(OH)+TMA): one –OH group bonded to the GaN surface with one TMA; **l**–**o** ($Ga_c(OH)_2$+TMA): two –OH groups bonded to the surface with one TMA introduced; **p**–**s** ($Ga_c(OH)_3$+TMA): three –OH groups bonded to the surface with one TMA introduced; **t**–**u** ($Ga_c(OH)_2$+2TMA): two –OH groups bonded to the surface with two TMA introduced, and **v**–**y** ($Ga_c(OH)_3$+2TMA)**:** three –OH groups bonded to the surface with two TMA introduced. For N_c GaN clusters, **z**(N_c(OH)+TMA)**:** one –OH group bonded to the GaN surface and **aa** ($N_c(OH)_3$+TMA): three –OH group bonded to the surface, while one TMA is introduced. For h_c GaN clusters, **ab**–**ad** (h_c(OH)+TMA): one –OH group bonded to the GaN surface with one TMA molecule introduced and **ae** ($h_c(OH)_2$+2TMA): two –OH group bonded to the surface with two TMA inserted molecules. O: red; osc: oscillatory convergence thus the structure failed to converge due to oscillations between two too near electronic states

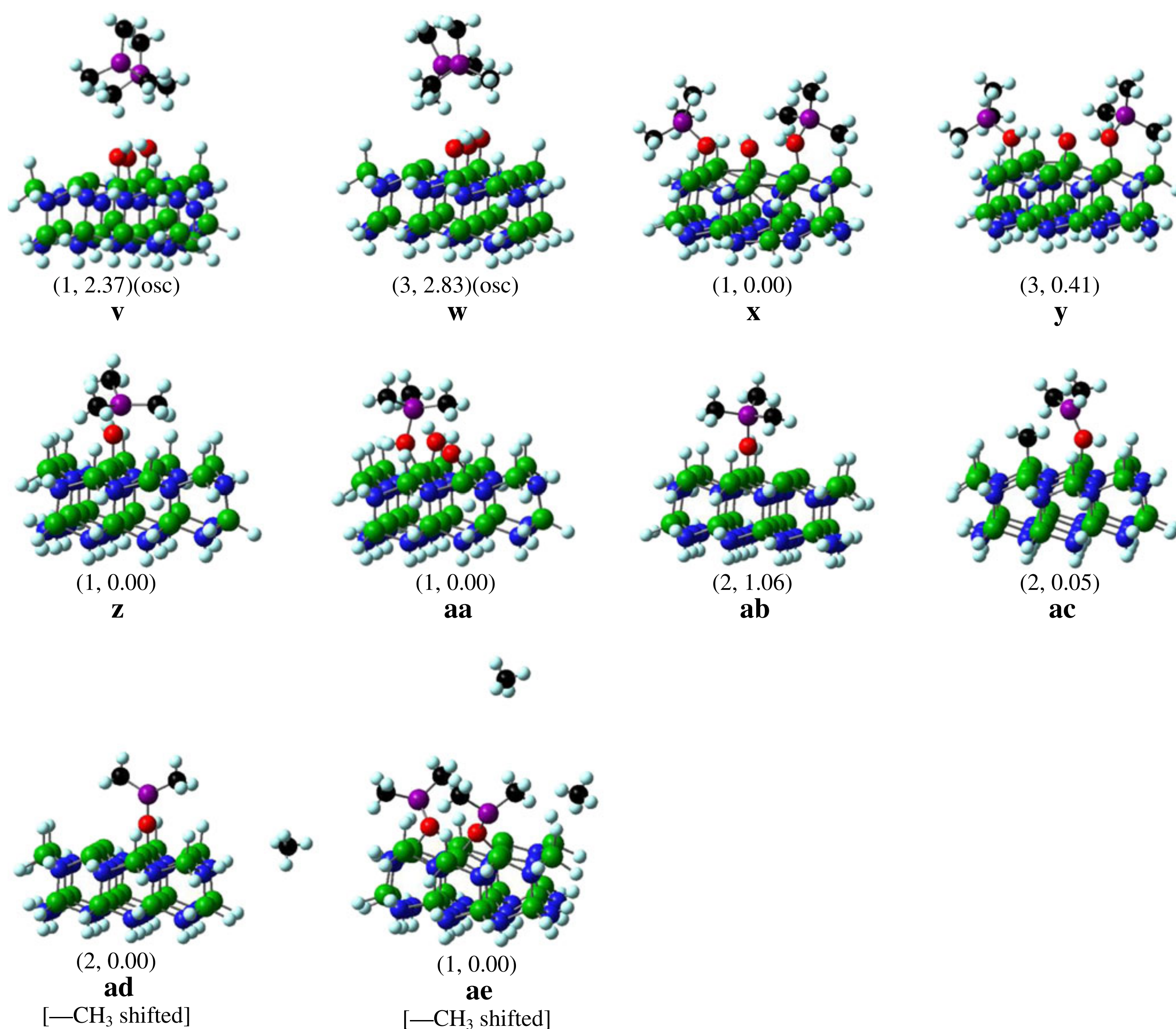

Fig. 3 (continued)

molecule that had been modified by breaking the Al—CH_3 bond. It is important to note the formation of a Ga-OH—Al bond accompanied by the formation of a Ga—CH_3 bond in **ac**. (Heretofore, we will be using "—" to refer to the specific bond under analysis). While the overall lowest energy is not obtained due to a sharp local minimum in the potential surface which causes the structure to oscillate in energy, the lowest energy is near the energy reported.

When two TMA molecules are placed over a double hydroxylated h_c cluster, $h_c(OH)_2$, and optimized (**ae**), the TMA is modified by shifting a CH_3 away from the Al and the only stable interaction of TMA with $h_c(OH)_2$, $h_c(OH)_2$+2TMA (**ae**), yields the formation of two O—Al bonds, two Ga-O—Ga bonds and two CH_4. This is the first time the formation of an O bonded to two surface Ga's and an Al has taken place within this study; however, due to the lack of another stable $h_c(OH)_2$+2TMA complex the only conclusion that can be drawn is that this structure may occur during the deposition process, it is not necessarily the most likely to occur.

The most common stable interactions between the hydroxylated GaN region and one or two TMA molecules generally leads to the formation of a Ga-OH—Al bond with only slight shifting of the bond lengths and angles of the Ga—O bonds, seen in **f**, **g**, **j**-**o**, **r**-**u**, **x**, **y**, **aa**, **ab** and **ac**. In the ALD of Al_2O_3 it is believed that O reacts with the Al to form a bond followed by the formation of CH_4. However, in this study it appears that the H prefers to remain bonded to the O rather than the CH_3. This could be due to the fact that under deposition conditions the reactants and substrate are heated to 250 °C thus increasing the kinetic energy of the molecules which may allow for the formation of CH_4, as seen in some of the modified TMA molecules in the complexes **h, ad** and **ae**. The modification

Table 1 Total optimized energies (E) for hydroxylated Ga_c, N_c and h_c GaN clusters interacting with 1 or 2 TMA, the number of –OH groups bonded to the GaN cluster, the number of TMA, energies of the initial (E_{RI}) and final (E_R) structures relative to the most stable conformation, the multiplicity (*m*) used, the initial (d_i) and final distances (d_f) from the O to the nearest Al, the formation of a CH_4 is determined and the shortest Ga-N bond length (d_{Ga-N}) for the Ga that is taking part in the reaction and the N that is part of the active region GaN

Structures (Fig. 3)		TMA	-OH	*m*	E (Ha)	E_{RI} (eV)	E_R (eV)	d_i (Å)	d_f (Å)	CH_4 formation?	d_{Ga-N} (Å)
Ga_c	f	1	1	1	−1471.13034	2.74	0.78	3.00	1.99	–	1.93
	g			3	−1471.11951	2.74	1.08	3.00	2.01	–	1.93
	h			1	−1471.15905	4.90	0.00	3.00	1.72	Yes	1.95
	i			1	−1471.09484	2.38	1.75	2.50	5.57	–	1.94
	j			1	−1471.13018	1.82	0.79	3.00	1.98	–	1.92
	k			3	−1471.11952	4.99	1.08	2.00	2.01	–	1.93
	l	1	2	2	−1547.02606	5.81	0.00	2.50	1.94	–	1.94
	m			4	−1547.01456	5.81	0.31	2.50	1.94	–	1.94
	n			2	−1546.99949	4.92	0.72	2.00	2.01	–	1.92
	o			4	−1546.98843	4.92	1.02	2.00	2.01	–	1.93
	p	1	3	1	−1622.88044[a]	4.29	0.60	3.60	4.05	–	1.96
	q			3	−1622.85887	4.29	1.19	3.60	4.13	–	1.95
	r			1	−1622.90255	9.45	0.00	2.50	1.99	–	1.94
	s			3	−1622.89368	9.45	0.24	2.50	1.95	–	1.94
	t	2	2	2	−1668.74865	11.62	0.00	1.50	1.99	–	1.93
	u			2	−1668.73673[b]	9.94	0.33	1.98	1.99	–	1.93
	v	2	3	1	−1744.55794[b]	7.07	2.47	2.70	4.41	–	1.95
	w			3	−1744.54447[b]	7.07	2.83	2.70	4.64	–	1.96
	x			1	−1744.64855	4.71	0.00	2.20	1.96	–	1.93
	y			3	−1744.63338	4.71	0.41	2.20	1.94	–	1.93
N_c	z	1	1	1	−1475.81611	3.88	0.00	2.00	2.03	–	1.93
	aa	1	3	1	−1627.57598	11.87	0.00	2.00	1.98	–	1.98
h_c	ab	1	1	2	−1587.84313	5.37	1.06	2.00	2.02	–	1.94
	ac			2	−1587.88016	10.75	0.05	1.45	1.90	–	1.76
	ad			2	−1587.88218	5.51	0.00	1.98	1.73	Yes	1.96
	ae	2	2	1	−1785.58088	15.27	0.00	1.98	1.82	Yes	1.89

[a] Imaginary frequencies (cm^{-1}): 94*i*

[b] oscillatory convergence

of TMA yields some of the most stable interactions for hydroxylated Ga_c (**h**) and h_c (**ad**) which form a Ga-O—Al bond and at least one CH_4, with a binding energy of −52.6 and −42.7 kcal mol^{-1}, respectively. These binding energies are some of the higher values for this type of interaction. The Al—O bond lengths of **h**, **ad**, **ae** (1.76 Å) are in good agreement, compared to 1.8 Å, with previously published data [65, 66]. It is important to mention the formation of a Ga-O—Ga bond where the O is bonded to Al geometry only occurs once throughout this research and is the only stable structure for the given complex.

Stability of the GaN-O—Al bond

The most stable TMA complex with a single, double or triple hydroxylated GaN cluster are used as the initial geometries to determine the stability of the O—Al bond over the GaN surfaces, Ga-O—Al$(CH_3)_2$ (Ga-O-dimethylaluminum (DMA)). These geometries are also used to determine the stability of the O—Al bond with other –OH groups or Ga—O bonds on GaN next to or near the O—Al bond (Fig. 4). The total energies are shown in Table 2 for the Ga_c, N_c, and h_c complexes.

Ga-centered GaN clusters (Ga_c) The stability of a single Ga-O—Al$(CH_3)_2$ geometry is tested using two different geometries bonded to the Ga_c cluster, Ga_c(O)-DMA (**af**, **ag**). The optimization of these geometries does not show deformation or degradation of any bonds in the complex (Ga_c(O)-DMA). The stability of the Ga-O—Al$(CH_3)_2$ geometry near an –OH group is tested using two geometries, Ga_c(OH)(O)-DMA (**ah**, **ai**). The most stable optimization yields the formation of a Ga-O—Al$(CH_3)_2$—O-Ga bond (**ah**). Finally the stability of two Ga-

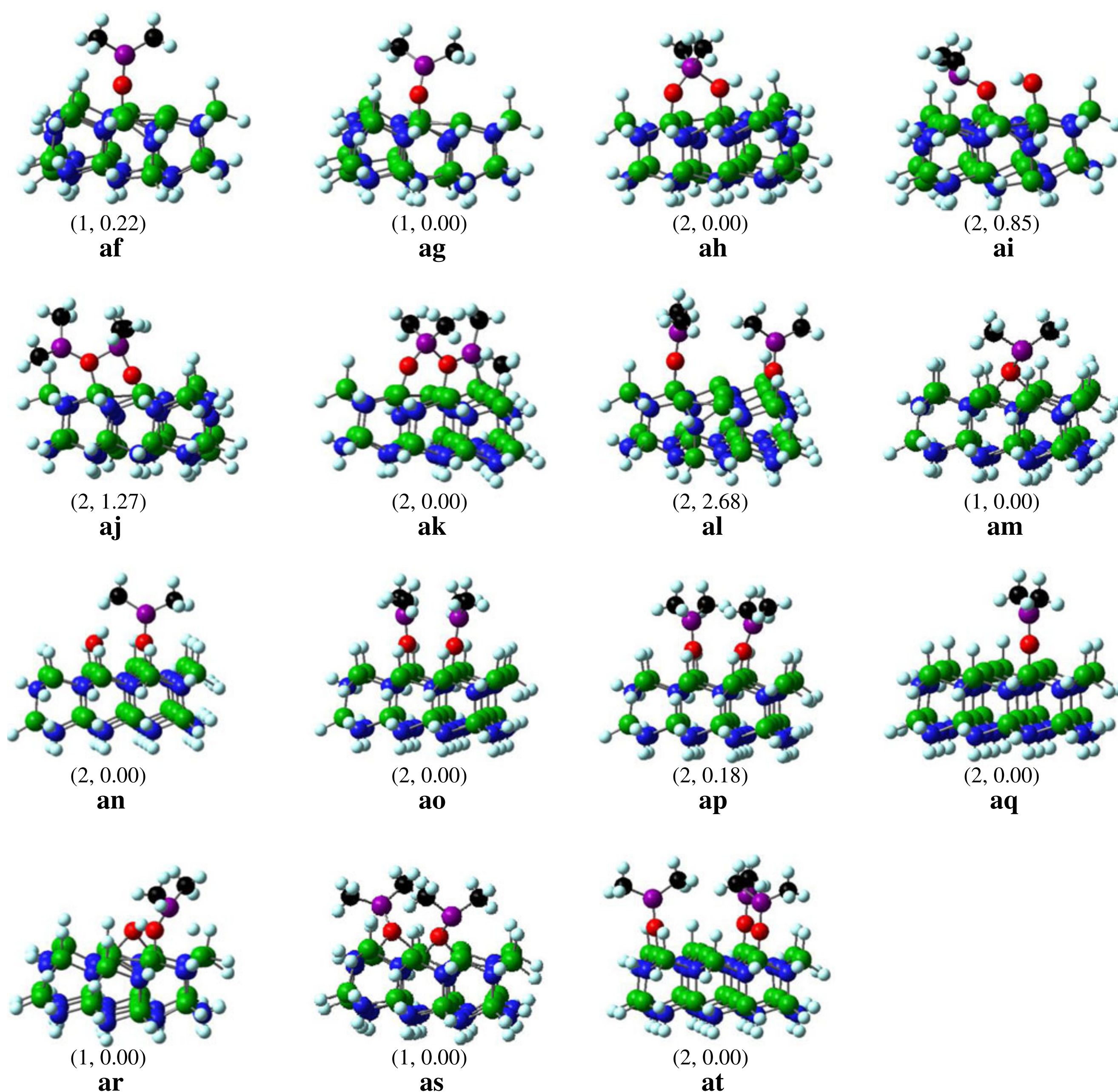

Fig. 4 Stability of 1, 2 or 3 reacted TMA (DMA) with formerly hydroxylated GaN clusters (partially H-passivated), now with 1, 2 or 3 Ga-O bonds, in some cases also in presence of remaining –OH group. The complexes are labeled with (m, E_R), indicating their spin multiplicity (m), and relative energy in eV (E_R) with respect to the most stable conformation, and bold letters; chemical changes with respect to their initial geometries are indicated inside square brackets. For Ga_c GaN clusters, **af-ag**(started from Ga_c(O)-DMA): one Al—O-Ga bond, **ah-ai**(Ga_c(OH)(O)-DMA): one Al—O-Ga bond and one –OH group bonded to the GaN and **aj-al(**Ga_c((O)-DMA)$_2$), two Al—O-Ga bonds have been optimized. For N_c GaN cluster, **am**(N_c(O)-DMA): one Al—O-Ga bond, **an(**N_c(OH)(O)-DMA): one Al—O-Ga bond and one –OH group bonded to the GaN surface and **ao-ap(**N_c((O)-DMA)$_2$): two Al—O-Ga bonds have been optimized. For h_c GaN cluster, **aq(**h_c(O)-DMA): one Al—O-Ga bond, **ar**(h_c(OH)(O)-DMA): one Al—O-Ga bond and one –OH group bonded to the GaN surface, **as**(h_c((O)-DMA)$_2$): two Al—O-Ga bonds, and **at**(h_c((O)-DMA)$_3$): three Al—O-Ga bonds have been optimized. O: red

O—Al$(CH_3)_2$ geometries on the Ga_c cluster is tested using three separate geometries, Ga_c((O)-DMA)$_2$ (**aj**-**al**). The overall most stable structure is Ga_c((O)-DMA)$_2$ (**ak**) which forms a Ga-O—Al$(CH_3)_2$—O-Ga bond and a Ga-O—AlCH_3—Ga bond with a Ga—CH_3 bond at the cluster edge. If there is an –OH group bonded to a surface Ga next to the Ga-O—Al$(CH_3)_2$ then the Al$(CH_3)_2$ shifts and binds with both O's. However, if the –OH group is not close enough, the Ga-O—Al$(CH_3)_2$ will remain unchanged.

N-centered GaN cluster (N_c) The stability of a single Ga-O—Al$(CH_3)_2$ geometry bonded to the N_c cluster is tested, N_c(O)-

Table 2 Total optimized energies (E) to evaluate the stability of reacted TMA (DMA) with formerly hydroxylated Ga_c, N_c and h_c GaN clusters, the number of –OH groups bonded to the GaN cluster, the number of DMA molecules, the number of O's bonded to the GaN cluster, energies of the initial (E_{RI}) and final (E_R) structures relative to the most stable conformation, the multiplicity (m) used, the initial (d_i) and final distances (d_f) from the O to the nearest Al, the formation of any new or broken bonds is determined and the shortest Ga-N bond length ($d_{Ga\text{-}N}$) for the Ga that is taking part in the reaction and the N that is part of the active region GaN

Structure (Fig. 4)		DMA	-OH	O	m	E (Ha)	E_{RI} (eV)	E_R (eV)	d_i (Å)	d_f (Å)	New/broken bonds?	$d_{Ga\text{-}N}$ (Å)
Ga_c	af	1	–	1	1	−1430.65807	0.24	0.22	1.72	1.72	–	1.95
	ag				1	−1430.66615	0.63	0.00	1.72	1.73	–	1.95
	ah	1	1	1	2	−1506.56724	1.09	0.00	1.72	1.78	Yes	1.93
	ai				2	−1506.53610	1.56	0.85	1.72	1.79	–	1.93
	aj	2	–	2	2	−1587.85405	9.11	1.27	1.72	1.81	Yes	1.93
	ak				2	−1587.90084	3.31	0.00	1.72	1.78	Yes	1.94
	al				2	−1587.80229	3.59	2.68	1.72	1.72	–	1.94
N_c	am	1	–	1	1	−1435.38572	1.15	0.00	1.72	1.93	Yes	1.95
	an	1	1	1	2	−1511.22984	1.24	0.00	1.72	1.73	–	1.97
	ao	2	–	2	2	−1592.50047	3.70	0.00	1.72	1.72	–	1.99
	ap				2	−1592.49980	3.48	0.02	1.72	1.72	–	1.99
h_c	aq	1	–	1	1	−1547.38087	0.24	0.00	1.72	1.72	–	1.95
	ar	1	1	1	2	−1623.25510	1.99	0.00	1.72	1.80	–	1.91
	as	2	–	2	1	−1704.57947	2.62	0.00	1.72	1.82	Yes	1.89
	at	3	–	3	2	−1861.68456	0.85	0.00	1.72	1.72	–	1.94

DMA (**am**). The optimization of this geometry yields the formation of a new Ga—O bond, where the O is bonded to two surface Ga's. The stability of the Ga-O—$Al(CH_3)_2$ geometry near an –OH group is tested in N_c(OH)(O)-DMA (**an**). The optimization does not show the formation or degradation of any bonds in the complex (N_c(OH)(O)-DMA). Finally the stability of two Ga-O—$Al(CH_3)_2$ geometries on the N_c cluster is tested using two separate geometries, $N_c((O)\text{-DMA})_2$ (**ao, ap**). The optimization does not show the formation or degradation of any bonds only slight shifts in bond lengths and angles of the initial geometry, Table 2.

Hollow-centered GaN clusters (h_c) The stability of a single Ga-O—$Al(CH_3)_2$ geometry bonded to the h_c cluster is tested, hc(O)-DMA (**aq**). The optimization does not reveal any formation or degradation of bonds of the complex (h_c(O)-DMA). The stability of the Ga-O—$Al(CH_3)_2$ geometry near an –OH group is tested, hc(OH)(O)-DMA (**ar**), and the optimization of this geometry yields the formation of a Ga—O bond showing an overall geometry of Ga-O—Ga and a floating H while the Ga-O—$Al(CH_3)_2$ geometry shifted in angle and in bond lengths. The stability of two Ga-O—$Al(CH_3)_2$ geometries on the hc cluster is tested using one geometry, $hc((O)\text{-DMA})_2$ (**as**). The optimization yields the formation of a Ga-O—Ga bond where the O is bonded to $Al(CH_3)_2$. The other Ga-O—$Al(CH_3)_2$ geometry shifted in angle and in bond lengths. Finally the stability of three Ga-O—$Al(CH_3)_2$ geometries on the h_c cluster is tested using one geometry, $hc((O)\text{-DMA})_3$ (**at**). The optimization does not result in the formation or degradation of any bonds only slight shifts in bond lengths and angles, Table 2.

Typically the Ga-O—$Al(CH_3)_2$ geometry is preserved during optimization if no other molecules are surrounding it (**af, ag, ai, al, aq** and **at**). However, in some cases the O or the $Al(CH_3)_2$ (DMA) shifts to form new bonds (**ah**, **aj, ak, am, ar** and **as**). For an example the Ga-O—$Al(CH_3)_2$ geometry on the N_c cluster, the O shifts to form a Ga-O—Ga bond without breaking any other bonds (**am**). It is important to note that due to the lack of multiple stable structures it is impossible to know if the structures shown here are the lowest energies achievable. However, some conclusions can be made. First, it is possible to form O—$Al(CH_3)_2$—O and Ga-O—Ga geometries during ALD of Al_2O_3 on GaN clusters. Second, the Ga-O—$Al(CH_3)_2$ geometry may interact with unreacted Ga—OH and other Ga-O—$Al(CH_3)_2$ geometries. Research is currently continuing in this area.

Tetrakis(ethylmethylamino) hafnium for deposition of hafnium oxide on gallium nitride

Interaction of TEMAH with hydroxylated GaN clusters

TEMAH is placed over a hydroxylated Ga_c and h_c GaN clusters to represent the atomic layer deposition (ALD) process of HfO_2 on GaN, Fig. 5. The total energies are shown in Table 3 for the Ga_c and h_c GaN complexes. The interaction of TEMAH with hydroxylated N_c cluster is tested; however, no stable structures are obtained.

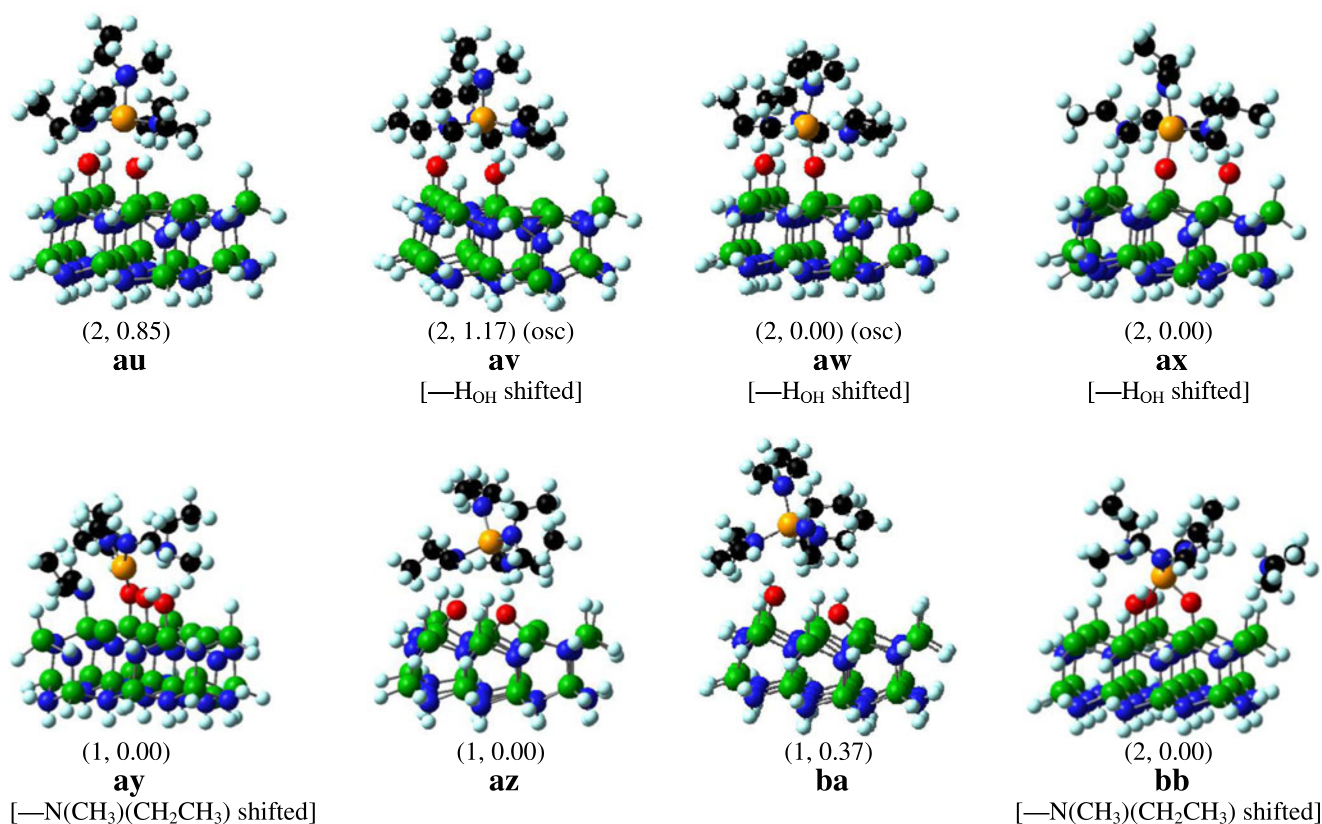

Fig. 5 GaN clusters (partially H-passivated) hydroxylated (with 2 or 3 –OH groups) optimized structures while under the presence of one TEMAH molecule. The complexes are labeled with (m, E_R), indicating their spin multiplicity (m), and relative energy in eV (E_R) with respect to the most stable conformation, and bold letters; chemical changes with respect to their initial geometries are indicated inside square brackets. For Ga_c GaN clusters, **au**(starting from $Ga_c(OH)_2$+TEMAH**)**: one TEMAH and two –OH groups, **av-ax(**$Ga_c(OH)_2$+TEMAH): two –OH groups and one TEMAH molecule, re-accommodating H atoms to avoid steric interactions, and **ay(**$Ga_c(OH)_3$+TEMAH): three –OH groups and one TEMAH with a N shifted. For hc GaN cluster**, az-ba(**$h_c(OH)_2$+TEMAH): two –OH groups and one TEMAH molecule and **bb(**$h_c(OH)_3$+TEMAH): three –OH groups and one TEMAH molecule with a N shifted. O: red, osc: failure to converge due to oscillations

Ga-centered GaN clusters (Ga_c) A single TEMAH molecule is placed over a double and triple hydroxylated Ga_c cluster, $Ga_c(OH)_2$ and $Ga_c(OH)_3$, respectively, in several orientations modifying bond lengths of C—H and N—Hf (from Hf—(N(CH$_3$)(CH$_2$CH$_3$))$_3$), and then optimized (**au-ay**). The most stable interaction yields the bonding of the TEMAH to the –OH group which caused Hf—N(CH$_3$)(CH$_2$CH$_3$) bond to break and react with the H from the –OH group forming an H—N bond (**aw-ay**). A shift in either the N—Hf bond or the O—H bond is necessary to form O—Hf and H—N(CH$_3$)(CH$_2$CH$_3$) bonds. Without shifting any atoms in the structure, the most stable structure between TEMAH and Ga_c(OH) resulted in a final relative energy (E_R) of 0.85 eV and no interaction between the hydroxylated surface and TEMAH (**au**).

Hollow-centered GaN clusters (h_c) One TEMAH molecule is placed over the double and triple hydroxylated h_c cluster, $h_c(OH)_2$ and $h_c(OH)_3$ in several orientations modifying bond lengths of C—H and N—Hf, and optimized (**az-bb**). The most stable interaction between TEMAH and the double hydroxylated h_c cluster yields the formation of a Ga-O—Ga bond without interacting with the TEMAH (**az**). The only stable interaction between TEMAH and the triple hydroxylated h_c cluster yields the bonding of the TEMAH to the –OH group which caused Hf—N(CH$_3$)(CH$_2$CH$_3$) bond to break and react with the H from the –OH group forming an H—N bond (**bb**). A shift in the N—Hf bond is necessary to form O—Hf and H—N(CH$_3$)(CH$_2$CH$_3$) bonds. The formation of H—N(CH$_3$)(CH$_2$CH$_3$) and O—Hf only occurs when either the Hf—N or the O—H bond lengths are increased significantly. Deposition temperatures of the substrate and TEMAH are around 200 °C and 150 °C, respectively. These temperatures correspond to increases in the kinetic energy of the molecules which leads to changes in bond lengths. The research shows that the most stable interaction between TEMAH and hydroxylated GaN clusters results in formation of H—N(CH$_3$)(CH$_2$CH$_3$) and Ga-O—Hf bonds **(aw, ax, ay, bb)**, when reaction kinetics allow, i.e., temperatures beyond that of room temperature; such structures have the most favorable binding energy, being for **ay** and **bb** of −61.4 and −56.4 kcal mol^{-1}, respectively. The Hf—O bond lengths of 2.02 Å for those molecules that formed N—H bonds, are similar to previously published data, 2.10 Å [67, 68].

Table 3 Total optimized energies (E) for hydroxylated Ga_c and h_c GaN cluster interacting with one TEMAH molecule, the number of –OH groups bonded to the GaN cluster, the number of TEMAH molecules, energies of the initial (E_{RI}) and final (E_R) structure relative to the most stable conformation, the multiplicity (m) used, the initial (d_i) and final distances (d_f) from the O to the nearest Hf, the formation of a N-H bond is determined and the shortest Ga-N bond length (d_{Ga-N}) for the Ga that is taking part in the reaction and the N that is part of the active region GaN. (Osc) signifies the structure failed to converge due to oscillations

Structure (Fig. 5)		TEMAH	-OH	m	E (Ha)	E_{RI} (eV)	E_R (eV)	d_i (Å)	d_f (Å)	N-H formation?	d_{Ga-N} (Å)
Ga_c	au	1	2	2	−2169.54182	15.57	0.85	2.40	2.47		1.94
	av			2	−2169.53025[a]	10.24	1.17	2.49	2.76		1.94
	aw			2	−2169.57318[a]	4.27	0.00	2.29	2.05	Yes	1.97
	ax			2	−2169.57321	2.34	0.00	2.71	2.05	Yes	1.97
	ay	1	3	1	−2245.51539	19.55	0.00	2.70	1.99	Yes	1.94
h_c	az	1	2	1	−2286.29151	15.07	0.00	3.28	3.99		1.89
	ba			1	−2286.27809	3.86	0.37	3.13	3.76		1.92
	bb	1	3	2	−2362.22714	30.02	0.00	2.00	1.98	Yes	1.96

[a] Oscillating convergence

It is important to mention the formation of a Ga-O—Ga bond where the O is bonded to Hf. This geometry only occurs once throughout this research and is the only stable structure for the given structure; therefore no definitive conclusions can be drawn.

Stability of the GaN-O—Hf bond

The most stable TEMAH interaction with a double hydroxylated GaN that matched the generally accepted initial structure O-Hf structure during ALD is used as

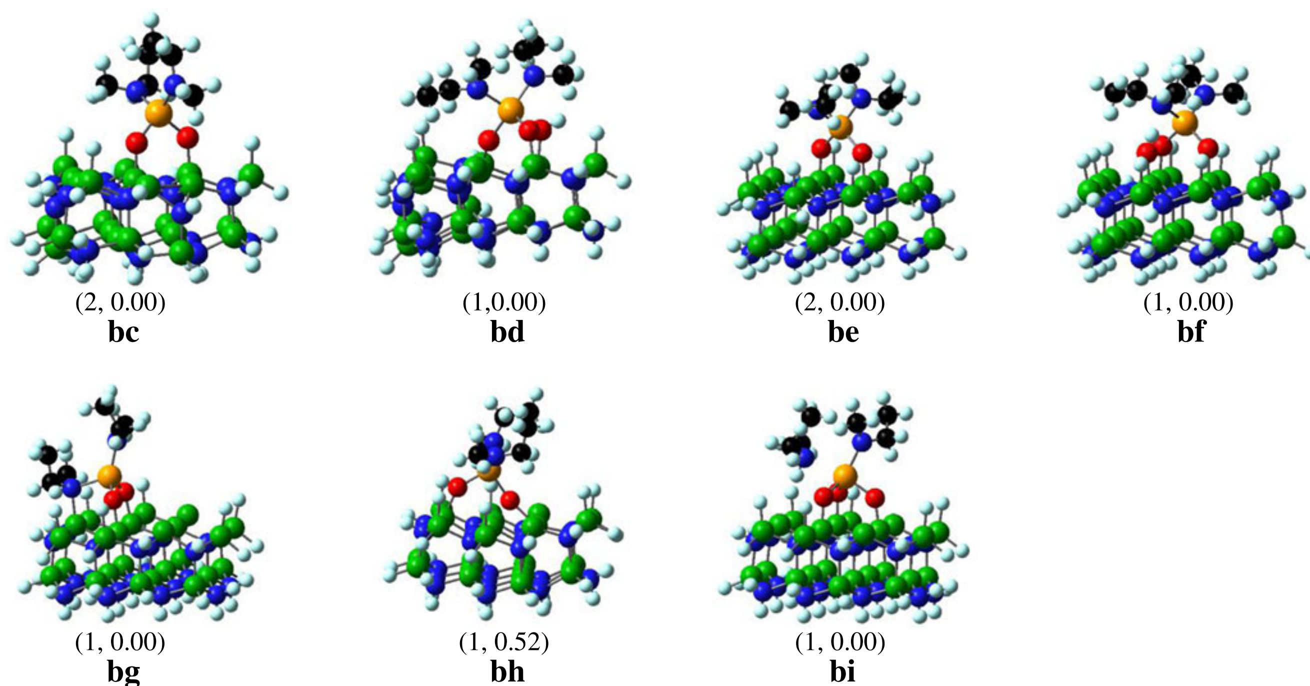

Fig. 6 Stability of one reacted TEMAH (HfAA) with formerly hydroxylated GaN clusters (partially H-passivated), now with 2 or 3 Ga-O bonds. TEMAH reacted on Ga-GaN clusters forming two O-Hf bonds, in some cases under the presence of one remaining –OH group. The complexes are labeled with (m, E_R), indicating their spin multiplicity (m), and relative energy in eV (E_R) with respect to the most stable conformation, and bold letters; chemical changes with respect to their initial geometries are indicated inside square brackets. For Ga_c GaN clusters, **bc** (started from $Ga_c(O)_2$-HfAA): one Ga-O—Hf($N(CH_3)(CH_2CH_3)$)$_2$—O-Ga bond and **bd**($Ga_c(OH)(O)_2$-HfAA): one Ga-O—Hf($N(CH_3)(CH_2CH_3)$)$_2$—O-Ga bond and one –OH group have been optimized. For N_c GaN clusters, **be**($N_c(O)_2$-HfAA): one Ga-O—Hf($N(CH_3)(CH_2CH_3)$)$_2$—O-Ga bond and **bf**($N_c(OH)(O)_2$-HfAA): one Ga-O—Hf($N(CH_3)(CH_2CH_3)$)$_2$—O-Ga bond and one –OH group have been optimized. For h_c GaN clusters, **bg-bh**($h_c(O)_2$-HfAA): one Ga-O—Hf($N(CH_3)(CH_2CH_3)$)$_2$—O-Ga bond, and **bi**($h_c(OH)(O)_2$-HfAA): one Ga-O—Hf($N(CH_3)(CH_2CH_3)$)$_2$—O-Ga bond and one –OH group have been optimized. O: red, Osc: complexes did not reach a minimum due to oscillations

Table 4 Total optimized energies (E) to evaluate the stability of reacted TEMAH(HfAA) with formerly hydroxylated Ga_c, N_c and h_c GaN cluster, the number of –OH groups bonded to the GaN cluster, the number of HfAA molecules, the number of O's bonded to the GaN cluster, energies of the initial (E_{RI}) and final (E_R) structure relative to the most stable conformation, the multiplicity (m) used, the initial (d_i) and final distances (d_f) from the O to the nearest Hf, the formation of new or broken bonds is determined and the shortest Ga-N bond length (d_{Ga-N}) for the Ga that is taking part in the reaction and the N that is part of the active region GaN

Structure (Fig. 6)		HfAA	-OH	O	m	E (Ha)	E_{RI} (eV)	E_R (eV)	d_i (Å)	d_f (Å)	New/broken bonds?	(d_{Ga-N}) (Å)
Ga_c	bc	1	–	2	2	−1820.82067	2.78	0.00	2.00	1.94	–	1.94
	bd	1	1	2	1	−1896.70358	5.60	0.00	2.00	1.96	–	1.90
N_c	be	1	–	2	2	−1825.51620	5.08	0.00	2.00	1.95	–	1.96
	bf	1	1	2	1	−1901.39807	7.10	0.00	2.00	1.93	–	1.95
h_c	bg	1	–	2	1	−1937.55161	4.72	0.00	2.00	1.90	Yes	1.92
	bh	1	–	2	1	−1937.53263	5.32	0.52	2.00	1.95	–	1.92
	bi	1	1	2	1	−2013.45498	4.18	0.00	2.00	1.97	Yes	1.96

the initial geometry to determine the stability of the O—Hf bond, over the hydroxylated GaN surfaces. Other geometries are also used to determine the stability of the O—Hf bond with other –OH groups or Ga—O bonds on GaN next to or near the O—Hf bond, Fig. 6. All complexes are optimized and the total energies are shown in Table 4 for the Ga_c, N_c, and h_c complexes.

Ga-centered GaN clusters (Ga_c) The stability of a single Hf—$(N(CH_3)(CH_2CH_3))_2$ (hafnium alkylamide (HfAA)) geometry, where the Hf is bonded to two O's, is tested with several geometries having the O atoms bonded to the Ga_c cluster; however the only complex that reaches a stable structure is $Ga_c(O)_2$-HfAA (**bc**). The geometry optimization of this complex does not show the formation or degradation of any bonds but only shows the shifting in bond angles and lengths of the complex (**bc**). The stability of the Hf—$(N(CH_3)(CH_2CH_3))_2$ geometry near an –OH group is tested, $Ga_c(OH)(O)_2$-HfAA (**bd**), and the most stable optimization yields the deformation and thus the upward bending of the GaN cluster (**bd**).

N-centered GaN clusters (N_c) While the interaction between hydroxylated N_c and TEMAH does not result in any stable structures, the stability of a single Hf—$(N(CH_3)(CH_2CH_3))_2$ geometry where the Hf is bonded to two O's is tested with the O's bonded to the N_c cluster, $N_c(O)_2$-HfAA (**be**). The optimization of this geometry does not show the formation or degradation of any bonds only shifts in bond angles and lengths of the complex $N_c(O)_2$-HfAA. The stability of the Hf—$(N(CH_3)(CH_2CH_3))_2$ geometry near an –OH group is tested, $N_c(OH)(O)_2$-HfAA (**bf**), and again the optimization of this geometry does not show the formation or degradation of any bonds only shifts in bond angles and lengths of the complex $N_c(OH)(O)_2$-HfAA (Table 4).

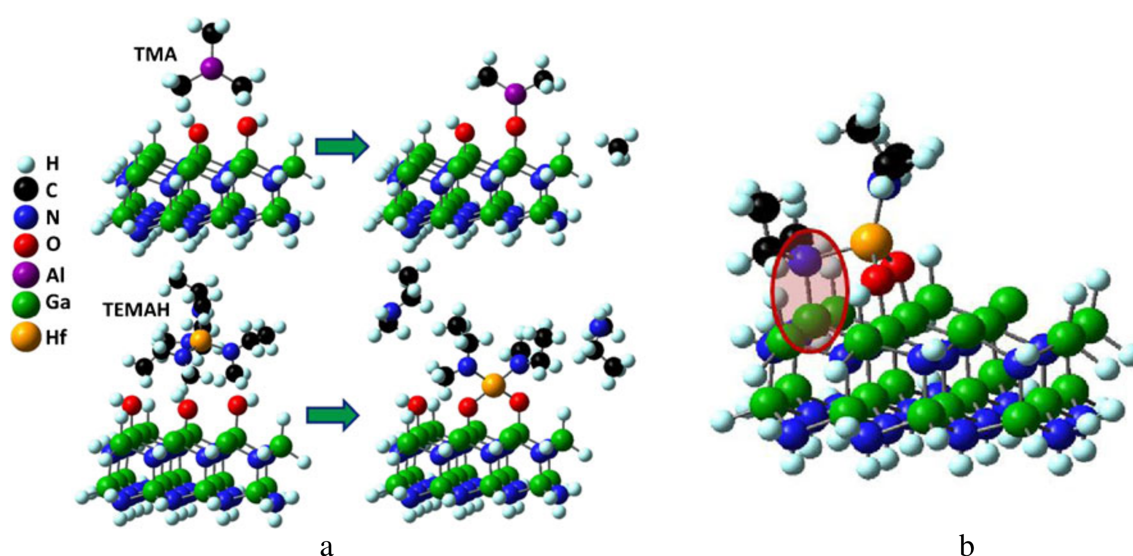

Fig. 7 **a** Interactions of TMA and TEMAH with hydrolyxated GaN clusters leading to the formation of CH_4, which is expected during the ALD process. **b** Formation of Ga—$N(CH_3)(CH_2CH_3)$ bond during deposition of HfO_2 using TEMAH forming the interfacial oxide during deposition of HfO_2 using ALD on GaN

Hollow-centered GaN clusters (h_c) The stability of a single Hf—$(N(CH_3)(CH_2CH_3))_2$ geometry where the Hf is bonded to two O's is tested using two geometries with the O's bonded to the h_c cluster, $h_c(O)_2$-HfAA (**bg**, **bh**). The optimization of this geometry, given the O's are attached to neighboring Ga surface atoms, yields the formation of a Ga—$N(CH_3)(CH_2CH_3)$ bond without breaking any bonds (**bg**) in the complex $h_c(O)_2$-HfAA. This interaction may be the mechanism behind the formation of interfacial layer during the ALD of HfO_2 on GaN. The optimization of a similar geometry with the O's separated by four Ga-N bond lengths does not show formation or degradation of any bonds, only shifts in bond angles and lengths (**bh**) of the complex $h_c(O)_2$-HfAA. The stability of the Hf—$(N(CH_3)(CH_2CH_3))_2$ geometry near an –OH group is tested, $h_c(OH)(O)_2$-HfAA (**bi**). The most stable optimization, results in the formation of a H—$N(CH_3)(CH_2CH_3)$ bond and an additional O—Hf bond (**bi**). It is important to note the formation of a stable Ga—$N(CH_3)(CH_2CH_3)$ bond (**bg**). While this geometry is the most stable, the **bh** is at only 0.52 eV above. Since the Ga—$N(CH_3)(CH_2CH_3)$ bond is only present in the most stable structure, this bonded structure may form during ALD of HfO_2 on GaN and may be the cause of the interfacial layer formation as no such structure is found in this research of TMA interacting with hydroxylated GaN clusters for fully optimized and stable structures.

It is important to note the formation of a stable Ga—$N(CH_3)(CH_2CH_3)$ bond (**bg**). While this geometry is the most stable, the **bh** is at only 0.52 eV above. Since the Ga—$N(CH_3)(CH_2CH_3)$ bond is only present in the most stable structure, this bonded structure may form during ALD of HfO_2 on GaN and may be the cause of the interfacial layer formation as no such structure is found in this research of TMA interacting with hydroxylated GaN clusters for fully optimized and stable structures.

Conclusions

Through this research, a better understanding of the interactions of TMA and TEMAH with hydroxylated GaN clusters during atomic layer deposition is achieved. TMA spontaneously interacts with hydroxylated GaN; however, the interaction does not result in the formation of a CH_4 which is expected during the ALD process. An increase in kinetic energy is needed to form methane and follow the expected Al_2O_3 ALD process. For the structures that formed a methane molecule, the O—Al bond lengths are similar to previously published works including Al_2O_3. In all other cases the most stable optimized geometries results in the TMA interacting with the hydroxylated GaN to form a Ga-O—Al bond. In one optimized structure, the formation of a Ga—CH_3 bond did occur. Similar to the interaction of TMA with hydroxylated GaN, TEMAH requires an increase in kinetic energy to follow the expected HfO_2 ALD process, e.g., the formation of a H—N bond. For the structures that formed a H—N bond, the O—Hf bond lengths are similar to previously published works including HfO_2. It is discovered that the formation of a Ga—$N(CH_3)(CH_2CH_3)$ bond can form during the deposition of HfO_2 using ALD and TEMAH as the reactant without breaking the Hf-N bond; this finding and the general procedure are schematically resumed in Fig. 7. The formation of a Ga—$N(CH_3)(CH_2CH_3)$ bond is significant because with the introduction of water into the complex the methyl and ethyl methyl groups may react to form a Ga-N—O bond which is believed to be the interfacial oxide found during deposition of HfO_2 using ALD on GaN.

Acknowledgments We acknowledge discussions with Prof. H. Rusty Harris, we also thank the Texas A&M Supercomputer Facility, and we acknowledge financial support from the U.S. Defense Threat Reduction Agency (DTRA) through the U.S. Army Research Office, project no. W91NF-06-1-0231, and ARO/MURI project no. W911NF-11-1-0024.

References

1. Koudymov A, Xuhong H, Simin K, Simin G, Ali M, Yang J, Asif Khan M (2002) Low-loss high power RF switching using multifinger AlGaN/GaN MOSHFETs. IEEE Electron Device Lett 23(8):449–451
2. Li G, Zimmermann T, Cao Y, Lain C, Xing X, Wang R, Fay P, Xing HG, Jena D (2010) Threshold voltage control in Al0.72Ga0.28N/AlN/GaN HEMTs by work-function engineering. IEEE Electron Device Lett 31(9):954–956
3. Yong C, Yugang Z, Lau KM, Chen KJ (2006) Control of threshold voltage of AlGaN/GaN HEMTs by fluoride-based plasma treatment: from depletion mode to enhancement mode. IEEE Trans Electron Devices 53(9):2207–2215
4. Guha S, Paruchuri VK, Copel M, Narayanan V, Wang YY, Batson PE, Bojarczuk NA, Linder B, Doris B (2007) Examination of flatband and threshold voltage tuning of HfO[sub 2]/TiN field effect transistors by dielectric cap layers. Appl Phys Lett 90(9):092902—1–3
5. Chang YC, Chiu HC, Lee YJ, Huang ML, Lee KY, Hong M, Chiu YN, Kwo J, Wang YH (2007) Structural and electrical characteristics of atomic layer deposited high κ HfO_2 on GaN. Appl Phys Lett 90(23):232904—1–3
6. Coan M, Johnson D, Woo JH, Biswas N, Misra V, Majhi P, Harris HR (2012) Work function extraction of metal gates with alternate channel materials. J Vac Sci Technol B 30(2):022202—1–5
7. Sivasubramani P, Park TJ, Coss BE, Lucero A, Huang J, Brennan B, Cao Y, Jena D, Xing H, Wallace RM, Kim J (2012) In-situ X-ray photoelectron spectroscopy of trimethyl aluminum and water half-cycle treatments on HF-treated and O_3-oxidized GaN substrates. Phys Status Solidi RRL 6(1):22–24. doi:10.1002/pssr.201105417
8. Chang YC, Huang ML, Chang YH, Lee YJ, Chiu HC, Kwo J, Hong M (2011) Atomic-layer-deposited Al_2O_3 and HfO_2 on GaN: a comparative study on interfaces and electrical characteristics. Microelectron Eng 88(7):1207–1210. doi:10.1016/j.mee.2011.03.098
9. Korbutowicz R, Prazmowska J, Wagrowski Z, Szyszka A, Taczaa M (2008) Wet thermal oxidation for GaAs, GaN and Metal/GaN device applications. In: Advanced semiconductor devices and microsystems, 2008. ASDAM 2008. International Conference on, 12–16 Oct. 2008. pp 163–166. doi:10.1109/asdam.2008.4743306
10. Readinger ED, Wolter SD, Waltemyer DL, Delucca JM, Mohney SE, Prenitzer BI, Giannuzzi LA, Molnar RJ (1999) Wet thermal oxidation

of GaN. J Elec Materi 28(3):257–260. doi:10.1007/s11664-999-0024-z
11. Hu C-L, Li J-Q, Zhang Y-F, Hu X-L, Lu N-X, Chen Y (2006) A DFT study of O_2 adsorption on periodic GaN (0001) and surfaces. Chem Phys Lett 424(4–6):273–278. doi:10.1016/j.cplett.2006.04.021
12. Hu C-L, Chen Y, Li J-Q (2009) First-principles calculations of H2O adsorption reaction on the GaN(0001) surface. Chin J Struct Chem 28(2):240–244
13. Coan MR, Leon-Plata P, Seminario JM (2012) Ab initio analysis of the interactions of GaN clusters with oxygen and water. J Phys Chem C 116(22):12079–12092. doi:10.1021/jp302026n
14. Nai-Xia L, Jun-Qian L, Yi-Jun X, Wen-Kai C, Yong-Fan Z (2004) Theoretical study of O_2 adsorption on GaN surfaces. J Mol Struct (THEOCHEM) 668(1):51–55. doi:10.1016/j.theochem.2003.10.005
15. Zywietz TK, Neugebauer J, Scheffler M (1999) The adsorption of oxygen at GaN surfaces. Appl Phys Lett 74(12):1695–1697
16. Seminario JM, Derosa PA, Cordova LE, Bozard BH (2004) A molecular device operating at terahertz frequencies. IEEE Trans Nanotechnol 3(1):215–218
17. Giovanni M (2002) Alloy nanoclusters in dielectric matrix. Nucl Inst Methods Phys Res B 191(1–4):323–332. doi:10.1016/s0168-583x(02)00527-x
18. Winter C, Kashammer J, Mittler-Neher S, Fischer RA (1998) A new pathway to GaN: deposition of GaN-clusters on functionalized thiol-SAMs on gold. Opt Mater 9(1–4):352–355. doi:10.1016/s0925-3467(97)00149-3
19. Bungaro C, Rapcewicz K, Bernholc J (2000) Ab initio phonon dispersions of wurtzite AlN, GaN, and InN. Phys Rev B 61(10):6720–6725
20. Nord J, Albe K, Erhart P, Nordlund K (2003) Modelling of compound semiconductors: analytical bond-order potential for gallium, nitrogen and gallium nitride. J Phys Condens Matter 15(32):5649–5662
21. Fritsch J, Sankey OF, Schmidt KE, Page JB (1998) Ab initio calculation of the stoichiometry and structure of the (0001) surfaces of GaN and AlN. Phys Rev B 57(24):15360–15371
22. Karch K, Wagner JM, Bechstedt F (1998) Ab initio study of structural, dielectric, and dynamical properties of GaN. Phys Rev B 57(12):7043–7049
23. Costales A, Pandey R (2003) Density functional calculations of small anionic clusters of Group III nitrides. J Phys Chem A 107(1):191–197. doi:10.1021/jp022202i
24. Song B, Yao C-H, P-l C (2006) Density-functional study of structural and electronic properties of Ga_nN (n=1-19) clusters. Phys Rev B 74(3):035306—1–8
25. Zhao J, Wang B, Zhou X, Chen X, Lu W (2006) Structure and electronic properties of medium-sized Ga_nN_n clusters (n=4–12). Chem Phys Lett 422(1–3):170–173. doi:10.1016/j.cplett.2006.02.048
26. Perez-Angel EC, Seminario JM (2011) Ab initio analysis and harmonic force fields of Gallium Nitride nanoclusters. J Phys Chem C 115(14):6467–6477. doi:10.1021/jp201004w
27. Hua-Gen Y (2011) An optimal density functional theory method for GaN and ZnO. Chem Phys Lett 512(4–6):231–236. doi:10.1016/j.cplett.2011.07.034
28. Brena B, Ojamäe L (2008) Surface effects and quantum confinement in nanosized GaN clusters: theoretical predictions. J Phys Chem C 112(35):13516–13523. doi:10.1021/jp8048179
29. Hohenberg P, Kohn W (1964) Inhomogeneous electron gas. Phys Rev B 136:864–871
30. Kohn W, Sham LJ (1965) Self-consistent equations including exchange and correlation effects. Phys Rev A 140:1133–1138
31. Becke AD (1993) Density-functional thermochemistry. III. The role of exact exchange. J Chem Phys 98(7):5648–5652
32. Roothaan CCJ (1951) New developments in molecular orbital theory. Rev Mod Phys 23(2):69–89
33. Pople JA, Nesbet RK (1954) Self-consistent orbitals for radicals. J Chem Phys 22(3):571–572
34. McWeeny R, Diercksen G (1968) Self-consistent perturbation theory. II. Extension to open shells. J Chem Phys 49(11):4852–4856
35. Perdew JP, Chevary JA, Vosko SH, Jackson KA, Pederson MR, Singh DJ, Fiolhais C (1993) Erratum: atoms, molecules, solids, and surfaces - applications of the generalized gradient approximation for exchange and correlation. Phys Rev B 48(7):4978–4978
36. Perdew JP, Chevary JA, Vosko SH, Jackson KA, Pederson MR, Singh DJ, Fiolhais C (1992) Atoms, molecules, solids, and surfaces: applications of the generalized gradient approximation for exchange and correlation. Phys Rev B 46(11):6671–6687
37. Perdew JP, Burke K, Wang Y (1996) Generalized gradient approximation for the exchange-correlation hole of a many-electron system. Phys Rev B 54(23):16533–16539
38. Perdew JP (1991) Unified theory of exchange and correlation beyond the local density approximation. In: Ziesche P, Eschrig H (eds) Electronic structure of solids. Akademie Verlag, Berlin, pp 11–20
39. Burke K, Perdew JP, Wang Y (1998) In: Ed JF, Dobson GV, Das MP (eds) Electronic density functional theory: recent progress and new directions. Plenum Press, New York
40. Cárdenas-Jirón GI, Leon-Plata P, Cortes-Arriagada D, Seminario JM (2011) Electrical characteristics of cobalt phthalocyanine complexes adsorbed on graphene. J Phys Chem C 115(32):16052–16062. doi:10.1021/jp2041026
41. Liuming Y, Eddy JB, Jorge MS (2007) Ab initio analysis of electron currents through benzene, naphthalene, and anthracene nanojunctions. Nanotechnology 18(48):485701—1–8
42. Fu M-L, Rangel N, Adams R, Seminario J (2010) Synthesis, crystal structure, photophysical properties, and DFT calculations of a Bis(tetrathia-calix[4]arene) Tetracadmium complex. J Clust Sci 21(4):867–878. doi:10.1007/s10876-010-0347-1
43. Seminario JM, Araujo RA, Yan L (2004) Negative differential resistance in metallic and semiconducting clusters. J Phys Chem B 108(22):6915–6918
44. Balbuena PB, Altomare D, Agapito LA, Seminario JM (2003) Theoretical analysis of oxygen adsorption on Pt-based clusters alloyed with Co, Ni, or Cr embedded in a Pt matrix. J Phys Chem B 107(49):13671–13680
45. Derosa PA, Seminario JM, Balbuena PB (2001) Properties of small bimetallic Ni-Cu clusters. J Phys Chem A 105(33):7917–7925
46. Zacarias AG, Castro M, Tour JM, Seminario JM (1999) Lowest energy states of small Pd clusters using density functional theory and standard ab initio methods. A route to understanding metallic nanoprobes. J Phys Chem A 103(38):7692–7700
47. Seminario JM, Zacarias AG, Castro M (1997) Systematic study of the lowest energy states of Pd, Pd_2, and Pd_3. Int J Quantum Chem 61:515–523
48. Seminario JM, Agapito LA, Yan L, Balbuena PB (2005) Density functional theory study of adsorption of OOH on Pt-based bimetallic clusters alloyed with Cr, Co, and Ni. Chem Phys Lett 410(4–6):275–281
49. Seminario JM, Tour JM (1997) Systematic study of the lowest energy states of Au_n (n=1-4) using DFT. Int J Quantum Chem 65:749–758
50. Seminario JM, Ma Y, Agapito LA, Yan L, Araujo RA, Bingi S, Vadlamani NS, Chagarlamudi K, Sudarshan TS, Myrick ML, Colavita PE, Franzon PD, Nackashi DP, Cheng L, Yao Y, Tour JM (2004) Clustering effects on discontinuous gold film NanoCells. J Nanosci Nanotechnol 4(7):907–917
51. Hay PJ, Wadt WR (1985) Ab initio effective core potentials for molecular calculations - potentials for the transition-metal atoms Sc to Hg. J Chem Phys 82(1):270–283
52. Hay PJ, Wadt WR (1985) Ab initio effective core potentials for molecular calculations - potentials for K to Au including the outermost core orbitals. J Chem Phys 82(1):299–310
53. Wadt WR, Hay PJ (1985) Ab initio effective core potentials for molecular calculations - potentials for main group elements Na to Bi. J Chem Phys 82(1):284–298

54. Seminario JM, Yan L (2005) Ab initio analysis of electron currents in thioalkanes. Int J Quantum Chem 102:711–723
55. Derosa PA, Guda S, Seminario JM (2003) A programmable molecular diode driven by charge-induced conformational changes. J Am Chem Soc 125:14240–14241
56. Seminario JM, De La Cruz C, Derosa PA, Yan L (2004) Nanometer-size conducting and insulating molecular devices. J Phys Chem B 108(46):17879–17885
57. Seminario JM, Yan L, Ma Y (2005) Scenarios for molecular-level signal processing. Proc IEEE 93(10):1753–1764
58. Peng C, Ayala PY, Schlegel HB, Frisch MJ (1996) Using redundant internal coordinates to optimize equilibrium geometries and transition states. J Comput Chem 17(1):49–56
59. Li X, Frisch MJ (2006) Energy-represented DIIS within a hybrid geometry optimization method. J Chem Theory Comput 2(3):835–839
60. Frisch MJ, Trucks GW, Schlegel HB, Scuseria GE, Robb MA, Cheeseman JR, Scalmani G, Barone V, Mennucci B, Petersson GA, Nakatsuji H, Caricato M, Li X, Hratchian HP, Izmaylov AF, Bloino J, Zheng G, Sonnenberg JL, Hada M, Ehara M, Toyota K, Fukuda R, Hasegawa J, Ishida M, Nakajima T, Honda Y, Kitao O, Nakai H, Vreven T, Montgomery J, J. A., Peralta JE, Ogliaro F, Bearpark M, Heyd JJ, Brothers E, Kudin KN, Staroverov VN, Kobayashi R, Normand J, Raghavachari K, Rendell A, Burant JC, Iyengar SS, Tomasi J, Cossi M, Rega N, Millam NJ, Klene M, Knox JE, Cross JB, Bakken V, Adamo C, Jaramillo J, Gomperts R, Stratmann RE, Yazyev O, Austin AJ, Cammi R, Pomelli C, Ochterski JW, Martin RL, Morokuma K, Zakrzewski VG, Voth GA, Salvador P, Dannenberg JJ, Dapprich S, Daniels AD, Farkas Ö, Foresman JB, Ortiz JV, Cioslowski J, Fox DJ (2009) Gaussian 09, Revision B.01. Gaussian Inc, Wallingford
61. Bougrov V, Levinshtein M, Rumyantsev S, Zubrilov A (2001) Gallium nitride (GaN). In: Levinshtein ME, Rumyantsev SL, Shur M (eds) Properties of advanced semiconductor materials : GaN, AlN, InN, BN, SiC, SiGe. Wiley, New York, pp 1–28
62. Halls MD, Raghavachari K (2004) Atomic layer deposition growth reactions of Al2O3 on Si(100)-2×1. J Phys Chem B 108(13):4058–4062. doi:10.1021/jp0378079
63. Puurunen RL (2005) Surface chemistry of atomic layer deposition: a case study for the trimethylaluminum/water process. J Appl Phys 97(12):121301–121352
64. Kim D-H, Baek S-B, Seo H-I, Kim Y-C (2011) Interactions between tri-methylaluminum molecules and their effect on the reaction of tri-methylaluminum with an OH-terminated Si (001) surface. Appl Surf Sci 257(15):6326–6331. doi:10.1016/j.apsusc.2011.01.032
65. Xu Y, Musgrave CB (2004) A DFT study of the Al2O3 atomic layer deposition on SAMs: effect of SAM termination. Chem Mater 16(4):646–653. doi:10.1021/cm035009p
66. Stierle A, Renner F, Streitel R, Dosch H, Drube W, Cowie BC (2004) X-ray diffraction study of the ultrathin Al_2O_3 layer on NiAl(110). Science 303(5664):1652–1656. doi:10.1126/science.1094060
67. Ren J, Zhang Y-T, Zhang DW (2007) Density functional theory study of initial stage of HfO_2 atomic layer deposition on hydroxylated SiO_2 surface. J Mol Struct (THEOCHEM) 803(1–3):23–28. doi:10.1016/j.theochem.2006.09.025
68. Robertson J, Peacock PW (2005) Atomic structure, interfaces and defects of high dielectric constant gate oxides. In: Demkov AA, Navrotsky A (eds) Materials fundamentals of gate dielectrics. Springer, Dordrecht, p 476. doi:10.1007/1-4020-3078-9_5